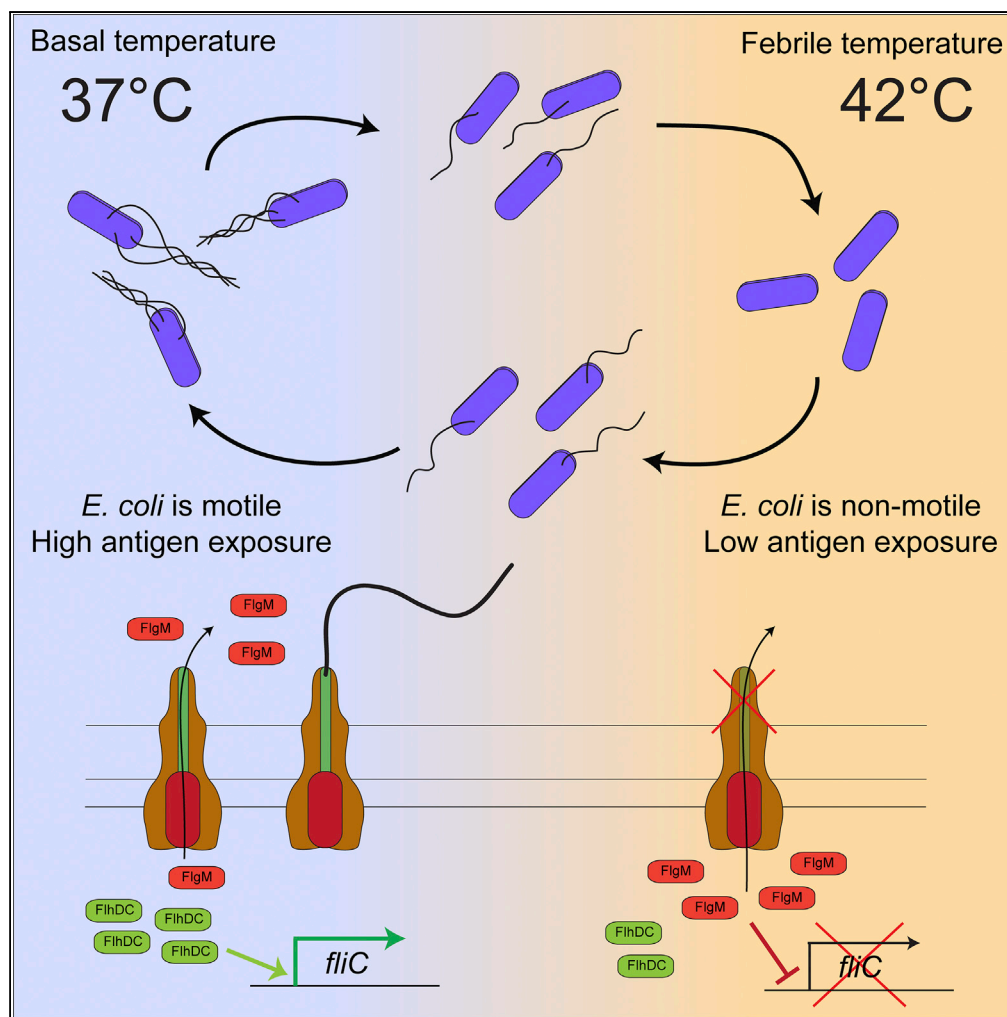Article

Inefficient Secretion of Anti-sigma Factor FlgM Inhibits Bacterial Motility at High Temperature

Iaroslav Rudenko,
Bin Ni, Timo
Glatter, Victor
Sourjik

victor.sourjik@synmikro.
mpi-marburg.mpg.de

HIGHLIGHTS
E. coli motility is tightly
turned off at febrile
temperature (42°C)

Repression of motility is
achieved at two levels of
hierarchical gene
regulation

Lowered FlhD level
reduces expression of all
flagellar genes

Impaired FlgM secretion
tightens repression of
class III genes

CellPress

Article

Inefficient Secretion of Anti-sigma Factor FlgM Inhibits Bacterial Motility at High Temperature

Iaroslav Rudenko,[1] Bin Ni,[1] Timo Glatter,[2] and Victor Sourjik[1,3,*]

SUMMARY

Temperature is one of the key cues that enable microorganisms to adjust their physiology in response to environmental changes. Here we show that motility is the major cellular function of *Escherichia coli* that is differentially regulated between growth at normal host temperature of 37°C and the febrile temperature of 42°C. Expression of both class II and class III flagellar genes is reduced at 42°C because of lowered level of the upstream activator FlhD. Class III genes are additionally repressed because of the destabilization and malfunction of secretion apparatus at high temperature, which prevents secretion of the anti-sigma factor FlgM. This mechanism of repression apparently accelerates loss of motility at 42°C. We hypothesize that *E. coli* perceives high temperature as a sign of inflammation, downregulating flagella to escape detection by the immune system of the host. Secretion-dependent coupling of gene expression to the environmental temperature is likely common among many bacteria.

INTRODUCTION

For microorganisms that proliferate in different environments, temperature is one of the most important environmental cues. Consequently, expression of several groups of genes that are important for survival within the host, including virulence genes, is regulated by temperature (Lam et al., 2014). But, although a majority of studies on the regulation of virulence genes were conducted in bacteria grown at 37°C, which is the normal temperature of their human host, the initiation of host immune response, followed by inflammation, commonly results in elevation of the body temperature up to 42°C, known as fever. Fever is common in mammal and other animals, and for many organisms, febrile temperature, 1°C–4°C above the basal level, correlates with efficient clearance of infection (Evans et al., 2015). The response of both pathogenic and commensal inhabitants of mammalian intestine to a moderate elevation of temperature that mimics fever could thus be potentially important for understanding bacterial response to inflammation. However, most of the studies of response of *E. coli* and other enterobacteria to high temperature focused on the heat shock conditions, corresponding to temperatures above 43°C (Roncarati and Scarlato, 2017; Rosen and Ron, 2002), which bacteria are unlikely to face inside the mammalian host.

One of the possible bacterial strategies of immune response evasion might be downregulation of strong antigens, such as flagella. Flagella are required for motility, which provides a number of advantages to bacterial cells, including access to nutrients and colonization of various environments (Ottemann and Miller, 1997). Because investment of resources in motility carries a high cost that can significantly affect cell growth (Ni et al., 2017), expression of motility genes is tightly regulated (Chevance and Hughes, 2008; Soutourina and Bertin, 2003). In the best-studied examples of *E. coli* and closely related *Salmonella* species, around 50 motility genes are hierarchically organized in three classes of expression (Chevance and Hughes, 2008). The environmental regulation of flagellar synthesis is believed to occur primarily at the level of the transcriptional regulator FlhDC (Pesavento et al., 2008; Soutourina and Bertin, 2003). The expression of *flhDC* operon (class I, early genes) is known to be controlled by a number of transcription factors. The level of FlhDC also depends on its degradation by the protease ClpXP (Kitagawa et al., 2011). FlhDC induces the expression of class II (middle) genes, which encode the components of flagellar hook-basal body (HBB), a sigma factor FliA, and an anti-sigma factor FlgM. FliA is required for the expression of class III (late) genes, which include the outer part of flagella, chaperones, and components of the chemotaxis pathway. The activity of FliA is negatively regulated by FlgM, which prevents FliA from activating class III promoters before complete assembly of the HBB. When the secretion system inside the basal body switches its export specificity (Hughes et al., 1993; Kutsukake et al., 1994), FlgM is secreted, thus liberating

[1]Department of Systems and Synthetic Microbiology, Max Planck Institute for Terrestrial Microbiology & LOEWE Center for Synthetic Microbiology (SYNMIKRO), Marburg 35043, Germany

[2]Core Facility for Mass Spectrometry & Proteomics, Max Planck Institute for Terrestrial Microbiology, Marburg 35043, Germany

[3]Lead Contact

*Correspondence: victor.sourjik@synmikro.mpi-marburg.mpg.de

https://doi.org/10.1016/j.isci.2019.05.022

FliA in the cell and enabling transcription of the class III genes followed by assembly of the outer part of flagellum, including filament cap and the filament itself (Guo et al., 2014; Macnab, 2004). FliA and FlgM, as well as several other flagellar genes, have both class II and class III promoters (Chilcott and Hughes, 2000; Fitzgerald et al., 2014).

The control of class III promoter activity by the interaction between FliA and FlgM is crucial for precise timing and extent of flagellar gene expression. Therefore, the concentrations of FliA and FlgM are regulated at multiple levels, with translation efficiency of *flgM* mRNA being dependent on the chaperone FlgN (Karlinsey et al., 2000), and FliA and FlgM being subject to proteolysis by the Lon and ClpXP proteases, respectively (Moliere et al., 2016). Finally, the secretion rate of FlgM is increased upon its binding to FliA and downregulated by its binding to the chaperone FliS (Aldridge and Hughes, 2002; Furukawa et al., 2016; Galeva et al., 2014; Guo et al., 2014). Such control of the motility system by the interplay between FliA and FlgM is relatively widespread among bacteria, including *Yersinia* (Ding et al., 2009), *Pseudomonas* (Hockett et al., 2013), *Vibrio* (Correa et al., 2004), and *Bacillus* (Calvo and Kearns, 2015) species.

The expression of motility genes in *E. coli* and other bacteria is known to depend on growth temperature, but underlying regulatory mechanisms are not well understood (Fahrner and Berg, 2015; Hockett et al., 2013; Horne and Pruss, 2006; Kamp and Higgins, 2011; Pruss, 2017; Shi et al., 1993; Wosten et al., 2010). Although FliA and/or FlgM have been implicated in temperature-dependent expression of flagellar genes in several species, including *Yersinia enterocolitica* (Horne and Pruss, 2006), *Pseudomonas syringae* (Hockett et al., 2013), and *Campylobacter jejuni* (Wosten et al., 2010), only in the latter case a mechanism, based on the thermosensitivity of the sigma-anti-sigma factor interaction, has been proposed.

Here we compared the transcriptome and proteome of *E. coli* grown at 37°C and at the febrile temperature 42°C. We observed that, in *E. coli* proteome, the motility system shows the most pronounced downregulation at 42°C. Our results suggest that such strong inhibition of motility occurs at two levels, partially due to the post-transcriptionally lowered level of FlhD, but primarily due to the malfunction of secretion apparatus at 42°C, which prevents secretion of FlgM and thereby inhibits the expression of class III genes. This regulation enables *E. coli* to highly efficiently turn off flagella expression at 42°C and turn them on again once the temperature is lowered back to 37°C. Given the wide spread of the FliA/FlgM control circuit among bacteria, this mechanism of thermoregulation is likely to be common, and it could explain previously observed temperature dependence of gene expression in *E. coli* and other bacteria (Hockett et al., 2013; Shi et al., 1993).

RESULTS AND DISCUSSION

Changes in Expression Induced at Febrile Temperature

To investigate response to fever temperature in *E. coli*, we first measured the mRNA and protein levels in cells grown at different temperatures. Increase of growth temperature from 37°C to 42°C resulted in differential regulation (at 90% confidence) of 127 genes and 119 proteins (Figure 1A, Tables S1 and S2). Similarly to several previous studies that compared regulation at the proteome and transcriptome levels (Borirak et al., 2015; Haider and Pal, 2013; Poblete-Castro et al., 2012), we observed an approximately 50% overlap between the two datasets. Consistently, there was a significant average correlation between changes in protein and mRNA levels (Figure 1B, Table S1), and also clear outliers that where differentially regulated, thus suggesting that response to 42°C occurs at both transcriptional and posttranscriptional levels. Of 66 genes downregulated at 42°C at both the mRNA and protein level (Table S2), the majority (40) were motility genes. Further 5 (*modA, modC, yecR, yjcZ, ynjH*) regulated genes were also reported to be under the control of FlhDC (Barbier et al., 2014; Fitzgerald et al., 2014; Horne and Pruss, 2006; Kapatral et al., 1996, 2004; Minnich and Rohde, 2007; Nuss et al., 2015; Shi et al., 1993). Also consistently downregulated were proteins involved in the catabolism of arginine (*astABCDE*), as well as anti-adaptor IraP responsible for stabilization of the stationary phase sigma factor RpoS (Bougdour et al., 2006). Upregulation on both levels at 42°C was observed for 13 genes, 5 of which (*rbsABCDK*) are involved in transport and metabolism of ribose. Several genes involved in the metabolism of iron (*fhuD, fhuE*) and carbohydrates (*gudD, malK, malP*), as well as a poorly characterized gene of the FlhDC regulon *flxA* (Ide and Kutsukake, 1997), showed opposite regulation on the protein and mRNA levels. Finally, six proteins were upregulated at 42°C at the protein but not on the mRNA level. Those included vertebrate lysozyme inhibitor Ivy and a multifunctional regulatory protein
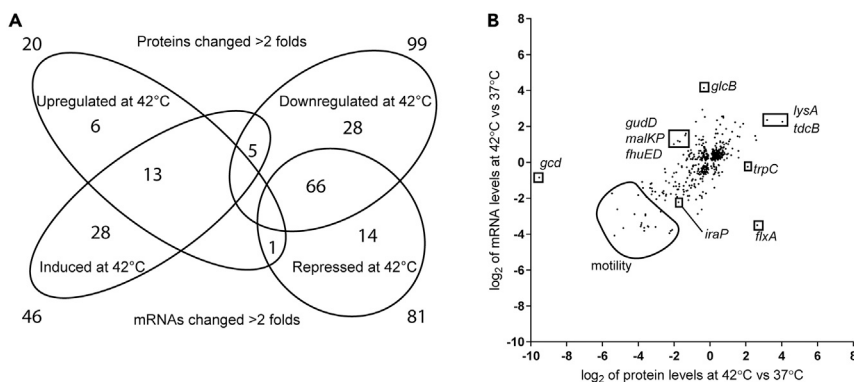
Figure 1. Changes in Transcriptome and Proteome between *E. coli* Grown at 37°C and 42°C

(A) Overlap between mRNAs and proteins showing more than 2-fold difference between 42°C and 37°C, determined, respectively, by RNA sequencing (RNA-seq) and mass spectrometry (see Methods). See also Table S1.

(B) Direct comparison of changes in the total transcriptome and proteome of cells grown at 42°C and 37°C. Genes and proteins with most pronounced regulation by growth temperature are highlighted. For both mRNA and protein, difference between $\log_2$ levels at 42°C and at 37°C is shown. Pearson correlation between regulation at the protein and mRNA levels, calculated for the shown dataset of 497 genes, is r = 0.6729, R^2 = 0.4528. See also Table S2.

StpA. Decreased protein levels at 42°C at unchanged mRNA levels were detected for 28 proteins, including RpoS, ribosome-associated RNA helicase RhlE, and transcriptional factors MhpR and MtlR involved in the metabolism of phenylpropionate and mannitol, respectively (Keseler et al., 2017). Decreased RpoS protein level at 42°C aligns well with the aforementioned decrease in the level of IraP as well as increased level of StpA, which was shown to inhibit translation of RpoS (Lucchini et al., 2009).

Temperature-Dependent Regulation of Flagellar Genes Occurs at Two Levels

To further investigate the observed strong downregulation of flagellar and motility genes at 42°C, we assessed the mRNA levels of different classes of flagellar genes over a wider range of temperature (Figures 2A–2D, Table S3). Consistently with an early report for *E. coli* (Shi et al., 1993), and also similar to the pattern observed for *Pseudomonas* and *Yersinia* (Barbier et al., 2014; Horne and Pruss, 2006; Kapatral et al., 1996, 2004; Minnich and Rohde, 2007; Nuss et al., 2015), the expression level of *flhDC* mRNA was nearly unaffected by temperature (Figure 2A, Table S4). The expression of class II genes showed a mild increase up to 37°C but decreased 2- to 4-fold at 42°C (Figure 2B). In contrast, expression of class III genes was strongly downregulated at 42°C, with up to a 16-fold drop in expression (Figure 2D and Table S3). Several genes having both class II and class III promoters showed intermediate regulation by temperature (Figure 2C). Notably, the overall pattern of class III flagellar gene expression was consistent with the previously reported temperature dependence of *E. coli* motility (Schulmeister et al., 2011).

As already observed in the global comparison of mRNA and protein levels (Figure 1B), relative changes in protein levels between 37°C and 42°C generally reflected regulation observed at the mRNA level, but with several notable differences (Figure 2E and Table S4). We observed that the level of FlhD was strongly reduced at 42°C, in contrast to constant levels of its mRNA. Oppositely, the levels of FliA and FlgM remained unchanged with growth temperature in spite of downregulation of their mRNAs at 42°C. Differences between protein and mRNA levels were also observed for several components of the ATPase, rod, hook, and P- and L-rings; some were more strongly and others more weakly downregulated at the protein level than at the mRNA level.

At least some of this differential regulation could be explained by differences in stability of respective proteins at 37°C and 42°C (Figures 3A–3D and S1). Although most flagellar proteins remained stable at both temperatures, the key component of the secretion apparatus FliP was less stable at 42°C, whereas chaperones FliS and FliT had increased decay rate at 37°C. Similarly, levels of FliA and FlgM were more stable at 42°C. Such stabilization is known to occur upon formation of the inhibitory FlgM-FliA complex (Galeva et al., 2014), which would also explain the repression of class III genes at 42°C. In contrast, degradation of FlhD was similar at both temperatures (Figures 3C and 3D), indicating that translational regulation rather
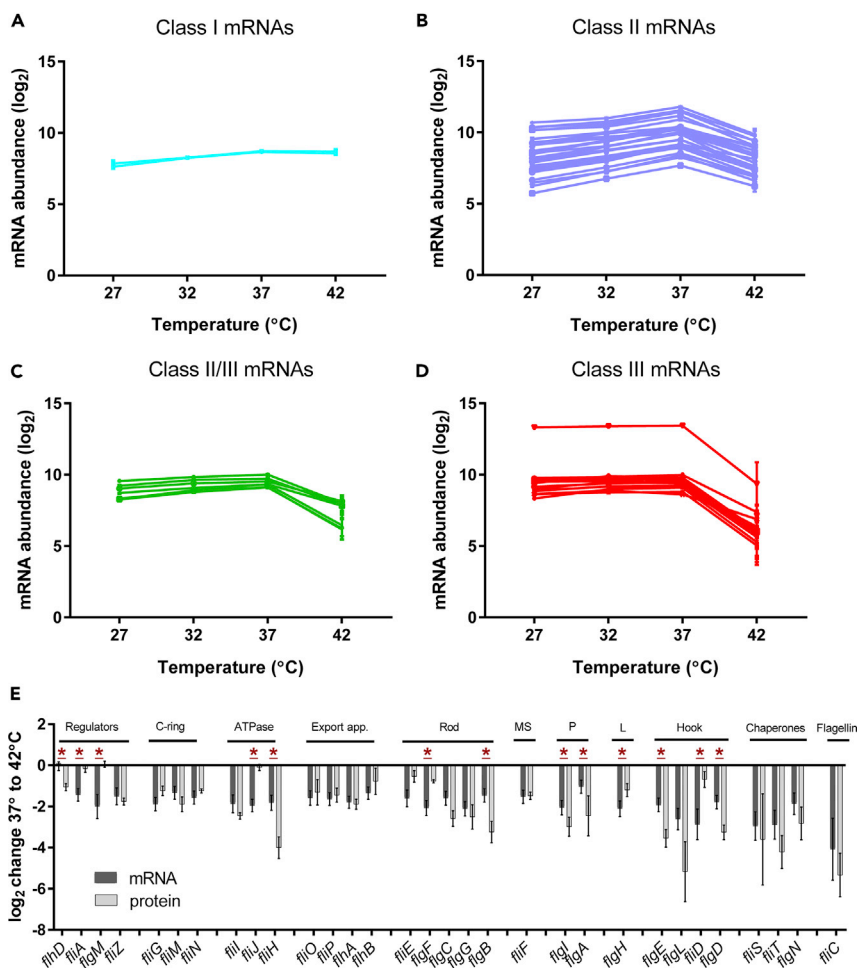
Figure 2. Growth Temperature Regulates Motility at mRNA and Protein Levels

(A–D) mRNA levels of class I (A), class II (B), class II/III (C), and class III (D) genes determined by RNA-seq at indicated growth temperatures. See also Table S3.

(E) Comparison of changes in the mRNA levels (from the data shown in A–D) and in the protein levels (determined by mass spectrometry, see Methods) between 42°C and 37°C. Indicated proteins are groups according to their function in the assembly of flagellum. Asterisks indicate significant difference between fold changes at the mRNA and protein levels according to the unpaired t test (p value < 0.015). Error bars in all panels show standard deviation for three independent experiments. See also Table S4.

that stability of FlhD is responsible for its lower levels at febrile temperature. Notably, reduced levels of flagellar proteins are consistent with absence of flagella from the cell surface (Figure 3E) and therefore with the lack of motility (Figure 3F) at 42°C.

To test the involvement of the FlgM-FliA interaction in the enhanced downregulation of *E. coli* class III genes at febrile temperature, we compared the activity of class II (*fliE*) and III (*fliC*) promoters at 37°C and 42°C in wild-type (WT) and *ΔflgM* strains (Figure 3G). Consistent with the transcriptomics results, in WT cells the activities of the class II and class III reporters decreased at 42°C to 20% and 2%, respectively. However, in the *ΔflgM* background the downregulation of both reporters was similar, confirming our hypothesis that enhanced repression of the class III genes at 42°C is mediated by FlgM. Since the increased formation of the FlgM-FliA complex might be due to the reduced secretion of FlgM at febrile temperature, we further compared intracellular and extracellular levels of FlgM at 37°C and 42°C, using FlgM that is C-terminally fused to a hemagglutinin (HA) tag (Ni et al., 2017) (see Transparent Methods). Although the concentration of cellular FlgM-HA was comparable at the two temperatures, consistent with the proteomic results, its level in the supernatant decreased dramatically at 42°C (Figure 3H). This drop seems to be a
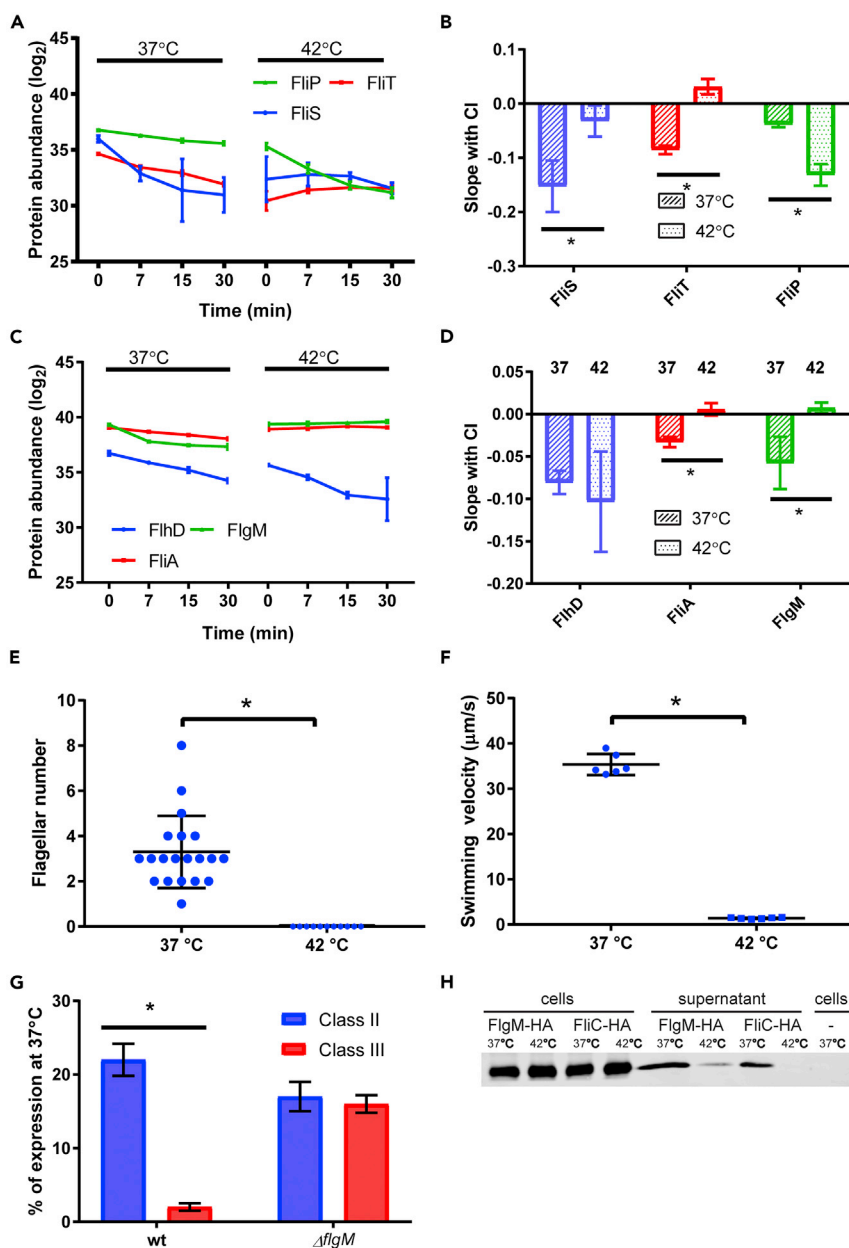
Figure 3. Growth Temperature Affects Stability of Transcriptional Regulators and Efficiency of Secretion Apparatus

(A) Time dependence of levels of most affected flagellum components after translation was stopped by addition of chloramphenicol to cultures grown at 37°C or 42°C. See also Figure S1.

(B) Decay rates of indicated proteins, calculated using linear fits to log data shown in (A). Each replicate was considered as an individual point. Asterisks indicate that linear fits are different with 95% confidence.

(C) Time dependence of levels of indicated regulators of flagellar gene expression after translation was stopped by addition of chloramphenicol to cultures grown at 37°C or at 42°C.

(D) Decay rates of indicated regulators, calculated using linear fits to log data shown in (C). Each replicate was considered as an individual point. Asterisks indicate that linear fits are different with 95% confidence.

(E) Number of flagella per cell in cells grown at 37°C or at 42°C detected by electron microscopy.

(F) Average swimming velocity as determined by cell tracking in cultures grown at 37°C or at 42°C.

(G) Relative activity of promotor reporters for class II (*fliE*) and class III (*fliC*) genes measured by flow cytometry in WT or in *ΔflgM* strain at 42°C. Activity was determined as GFP fluorescence, with values at 42°C normalized to those at 37°C. Error bars in all panels show standard deviation for at least three independent experiments. Asterisks in panels E–G indicate significant differences between samples according to the unpaired t test (p value < 0.01).

Figure 3. *Continued*

(H) Immunoblot analysis of FlgM-HA and FliC-HA levels inside cells and in the culture supernatant at 37°C and 42°C. Tagged proteins were expressed from the IPTG-inducible plasmid (see Methods). Negative control (indicated by "-") shows sample of cells without the plasmid.

consequence of the general failure of the secretion system at febrile temperature, since essentially the same result was obtained with the HA-tagged fusion to the fragment of FliC (Ni et al., 2017). Such impaired secretion of flagellin and other late substrates of the export apparatus could explain stabilization of their chaperones FliS and FliT.

Flagellar Secretion Apparatus Is Destabilized at High Temperature

To further test the integrity of the secretion apparatus at 42°C, we used cyan and yellow fluorescent protein fusions to FlhA (component of the export apparatus; FlhA-CFP) and FliF (MS ring component of the basal body; FliF-YFP). These two proteins are known to initiate assembly of the flagellar motor in *E. coli* (Li and Sourjik, 2011). Expectedly, at 37°C both fusions localized to basal bodies, visible as multiple lateral fluorescent foci along the cellular periphery (Figure 4A). We observed that, at increased temperature, the number and intensity of lateral FlhA-CFP foci became largely reduced, with fusion protein mostly accumulating in polar aggregates, whereas the levels of full-length fusion proteins remained similar (Figures 4A, 4B, S2, and S3). The reduction of lateral foci was similarly pronounced for FliF-YFP. Such delocalization of the key components of the basal body and secretion apparatus indicates that the machinery is at least partly disassembled during growth at 42°C. In contrast, in the absence of cell growth already assembled MS rings appear to be stable for at least 60 min at 42°C. Localization of FlhA-CFP moderately decreased under these conditions (Figures S4 and S5), which is consistent with the previously observed faster exchange of FlhA at the HBB compared with FliF (Li and Sourjik, 2011). These results suggest that high growth temperature directly destabilizes the export apparatus by weakening the assembly of its early components FliF and FlhA.

Taken together, we could show that an elevated growth temperature (42°C) affects the motility system of *E. coli* in several ways (Figure 4C). Although the level of *flhD* mRNA was nearly unaffected by temperature, the level of FlhD protein was significantly reduced. Although this decrease can explain the weakly reduced activity of class II promoters at 42°C, the dramatic downregulation of class III genes is primarily caused by the inhibited secretion of the anti-sigma factor FlgM and the ensuing inhibition of FliA activity. This failure of the secretion apparatus is apparently the consequence of its reduced assembly at high growth temperature, which may be caused by a combination of direct temperature effects on the HBB structure (i.e., weakened interactions between its components) and decreased levels of class II gene products that stabilize the early steps of the HBB self-assembly (Li and Sourjik, 2011).

Changes of Motility upon Temperature Shifts Are Gradual

We further investigated how motility changed over time when growth temperature of the culture was shifted from 37°C to 42°C (Figures 5A and 5B) or from 42°C to 37°C (Figures 5C and 5D). For both shifts only gradual reduction, or, respectively, increase, was observed, not only on the level of GFP expression but also when directly analyzing cell motility. The former could be explained by high stability and maturation times of GFP, meaning that its levels need to be reduced by cell division or take time to build up, even upon the rapid change in transcription. Similarly slow changes in motility suggest that also flagella are not rapidly shed off at 42°C but rather gradually diluted, most likely by growth, and that biogenesis of complete flagella requires more than 1 h, consistent with the previous work (Renault et al., 2017). Importantly, we observed that the WT cells required less time to adjust motility to the new steady-state level than *ΔflgM* cells, suggesting that the FlgM-mediated negative regulation shortens these transitions. For both upshift and downshift of temperature, motility of the WT cells largely equilibrated within 90–120 min, whereas in the *ΔflgM* strain, motility continued to increase gradually throughout the time course of the experiment, up to 150 min (Figures 5B and 5D). A similar pattern was observed for the promoter reporter activity upon shift from 42°C to 37°C (Figure 5C).

Conclusions

Overall, here we show that flagellar motility is the major cellular function that is downregulated by *E. coli* upon transition to the febrile temperature. Such loss of motility might be beneficial for survival of *E. coli* during inflammation in the host, as on one hand flagella are strongly antigenic and reducing their number might
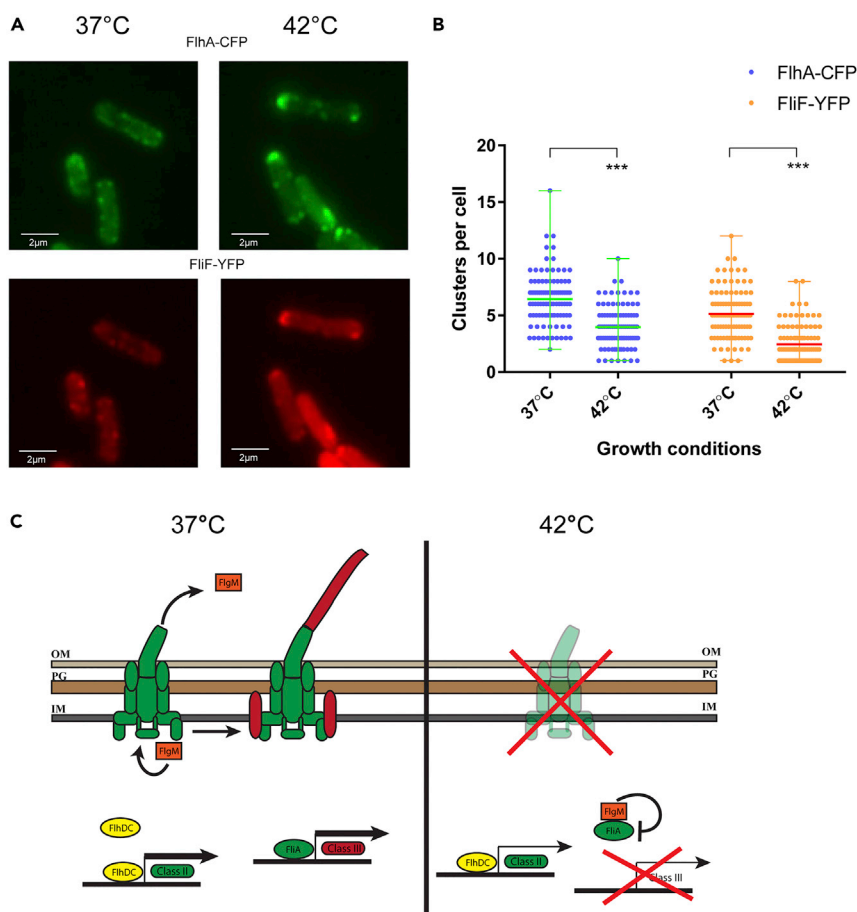
Figure 4. Effect of Temperature on Assembly of MS Ring and Secretion Apparatus

(A) Localization of FlhA-CFP and FliF-YFP (expressed from respective inducible plasmids, see Methods) at 37°C (left) and at 42°C (right). See also Figure S2.

(B) Quantification of the number of visible FlhA-CFP or FliF-YFP clusters per cell at 37°C and 42°C. For each construct, clusters were blind counted in 100 cells from 10 images, originating from two independent experiments done as in A. Wide horizontal lines indicate the median. Asterisks indicate p value < 0.0001 (Mann-Whitney test, see Methods). See also Figures S3–S5.

(C) Schematics of the proposed mechanism of downregulation of motility at high growth temperature. At 37°C (left), FlhDC is stable, class II genes (green) are expressed, basal body is assembled, and FlgM is secreted from the cell. Consequently, FliA induces expression of class III genes (red), required for the assembly of the outer part of the flagellum. At 42°C (right), the FlhDC level decreases, the basal body is unstable/misassembled, and FlgM secretion is impaired. Formation of FlgM-FliA complex prevents activation of the class III genes.

facilitate evasion of the activated immune response and on the other hand motility might be important for competition with other species and colonization of the host (Siryaporn et al., 2015). We observed that the downregulation of *E. coli* flagellar gene expression at high temperature occurs at two levels: First, transcription of all class II and class III genes is reduced several-fold due to the lowered level of FlhD. This reduction in protein level occurs in the absence of transcriptional regulation of *flhD* and is most likely explained by the temperature dependence of translation. Second, repression of class III genes is largely enhanced because of inhibited secretion of FlgM at 42°C, caused by destabilization and failure of the secretion apparatus. Although both loss and reacquisition of motility upon changes in growth temperature are relatively slow and likely driven by growth-dependent dilution and resynthesis of flagella, the FlgM-mediated negative regulation apparently accelerates transition to the new steady state. Finally, our observations could explain the previously reported expression pattern of *E. coli* motility and flagellar gene expression at high temperature (Shi et al., 1993). The selective repression of class III genes via inhibited secretion of FlgM is also likely to control flagellar gene expression at elevated temperature in bacteria other than *E. coli*, explaining the
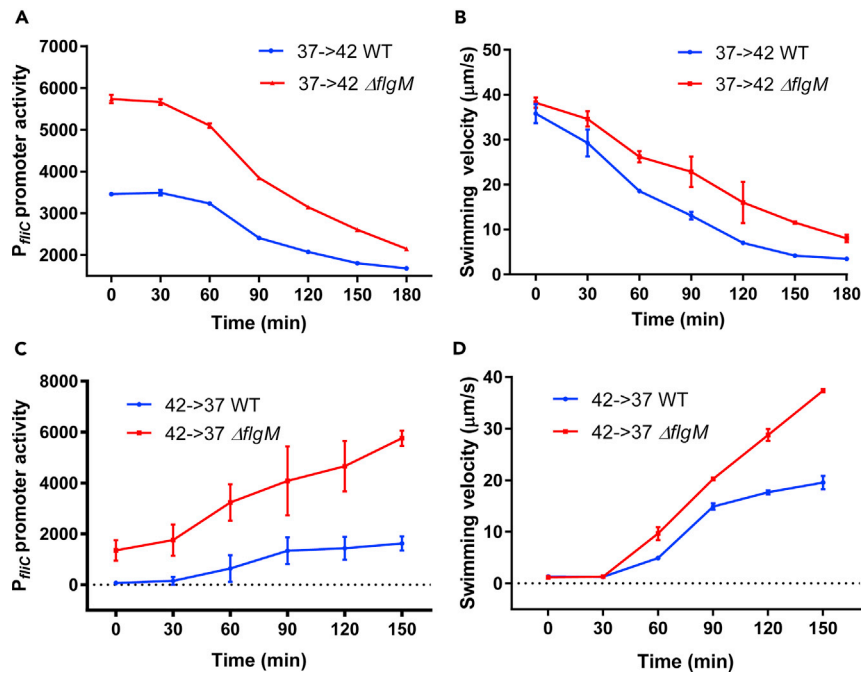
Figure 5. Changes of Class III Gene Expression and Motility upon Upshift or Downshift of Temperature

(A and B) Relative activity of promotor reporter for the class III gene (*fliC*; A) and of cell swimming velocity (B) upon shift of the growth temperature from 37°C to 42°C. Promoter activity was measured as GFP fluorescence by flow cytometry and motility was determined by cell tracking (see Methods) in WT or in *ΔflgM* strain, as indicated.

(C and D) Same as (A and B) but for the growth temperature shift from 42°C to 37°C. Error bars in all panels show standard deviation for three independent experiments.

thermoregulation of flagellar genes observed in species such as *Y. enterocolitica* (Horne and Pruss, 2006; Kapatral et al., 2004) and *P. syringae* (Hockett et al., 2013).

Limitations of the Study

Although our data indicate that FlhD is downregulated at 42°C at the translational level, the mechanism of the underlying regulation remains to be understood. Furthermore, our study did not allow us to determine the causal relationship between destabilization of flagellar basal body and enhanced degradation of its components at elevated temperature.

METHODS

All methods can be found in the accompanying Transparent Methods supplemental file.

SUPPLEMENTAL INFORMATION

Supplemental Information can be found online at https://doi.org/10.1016/j.isci.2019.05.022.

AUTHOR CONTRIBUTIONS

V.S. and I.R. designed experiments; I.R. and B.N. performed experiments; I.R. and T.G. analyzed the data; V.S. and I.R. wrote the manuscript.

DECLARATION OF INTERESTS

The authors declare no competing interests.

REFERENCES

Aldridge, P., and Hughes, K.T. (2002). Regulation of flagellar assembly. Curr. Opin. Microbiol. *5*, 160–165.

Barbier, M., Damron, F.H., Bielecki, P., Suárez-Diez, M., Puchałka, J., Albertí, S., dos Santos, V.M., and Goldberg, J.B. (2014). From the environment to the host: re-wiring of the transcriptome of *Pseudomonas aeruginosa* from 22°C to 37°C. PLoS One *9*, e89941.

Borirak, O., Rolfe, M.D., de Koning, L.J., Hoefsloot, H.C., Bekker, M., Dekker, H.L., Roseboom, W., Green, J., de Koster, C.G., and Hellingwerf, K.J. (2015). Time-series analysis of the transcriptome and proteome of *Escherichia coli* upon glucose repression. Biochim. Biophys. Acta *1854*, 1269–1279.

Bougdour, A., Wickner, S., and Gottesman, S. (2006). Modulating RssB activity: IraP, a novel regulator of sigma(S) stability in *Escherichia coli*. Gene Dev. *20*, 884–897.

Calvo, R.A., and Kearns, D.B. (2015). FlgM is secreted by the flagellar export apparatus in *Bacillus subtilis*. J. Bacteriol. *197*, 81–91.

Chevance, F.F., and Hughes, K.T. (2008). Coordinating assembly of a bacterial macromolecular machine. Nat. Rev. Microbiol. *6*, 455–465.

Chilcott, G.S., and Hughes, K.T. (2000). Coupling of flagellar gene expression to flagellar assembly in *Salmonella enterica* serovar Typhimurium and *Escherichia coli*. Microbiol. Mol. Biol. Rev. *64*, 694–708.

Correa, N.E., Barker, J.R., and Klose, K.E. (2004). The Vibrio cholerae FlgM homologue is an anti-sigma28 factor that is secreted through the sheathed polar flagellum. J. Bacteriol. *186*, 4613–4619.

Ding, L., Wang, Y., Hu, Y., Atkinson, S., Williams, P., and Chen, S. (2009). Functional characterization of FlgM in the regulation of flagellar synthesis and motility in *Yersinia pseudotuberculosis*. Microbiology *155*, 1890–1900.

Evans, S.S., Repasky, E.A., and Fisher, D.T. (2015). Fever and the thermal regulation of immunity: the immune system feels the heat. Nat. Rev. Immunol. *15*, 335–349.

Fahrner, K.A., and Berg, H.C. (2015). Mutations that stimulate flhDC expression in *Escherichia coli* K-12. J. Bacteriol. *197*, 3087–3096.

Fitzgerald, D.M., Bonocora, R.P., and Wade, J.T. (2014). Comprehensive mapping of the *Escherichia coli* flagellar regulatory network. PLoS Genet. *10*, e1004649.

Furukawa, Y., Inoue, Y., Sakaguchi, A., Mori, Y., Fukumura, T., Miyata, T., Namba, K., and Minamino, T. (2016). Structural stability of flagellin subunit affects the rate of flagellin export in the absence of FliS chaperone. Mol. Microbiol. *102*, 405–416.

Galeva, A., Moroz, N., Yoon, Y.H., Hughes, K.T., Samatey, F.A., and Kostyukova, A.S. (2014). Bacterial flagellin-specific chaperone FliS interacts with anti-sigma factor FlgM. J. Bacteriol. *196*, 1215–1221.

Guo, S., Alshamy, I., Hughes, K.T., and Chevance, F.F. (2014). Analysis of factors that affect FlgM-dependent type III secretion for protein purification with *Salmonella enterica* serovar Typhimurium. J. Bacteriol. *196*, 2333–2347.

Haider, S., and Pal, R. (2013). Integrated analysis of transcriptomic and proteomic data. Curr. Genomics *14*, 91–110.

Hockett, K.L., Burch, A.Y., and Lindow, S.E. (2013). Thermo-regulation of genes mediating motility and plant interactions in *Pseudomonas syringae*. PLoS One *8*, e59850.

Horne, S.M., and Pruss, B.M. (2006). Global gene regulation in *Yersinia enterocolitica*: effect of FliA on the expression levels of flagellar and plasmid-encoded virulence genes. Arch. Microbiol. *185*, 115–126.

Hughes, K.T., Gillen, K.L., Semon, M.J., and Karlinsey, J.E. (1993). Sensing structural intermediates in bacterial flagellar assembly by export of a negative regulator. Science *262*, 1277–1280.

Ide, N., and Kutsukake, K. (1997). Identification of a novel *Escherichia coli* gene whose expression is dependent on the flagellum-specific sigma factor, FliA, but dispensable for motility development. Gene *199*, 19–23.

Kamp, H.D., and Higgins, D.E. (2011). A protein thermometer controls temperature-dependent transcription of flagellar motility genes in *Listeria monocytogenes*. PLoS Pathog. *7*, e1002153.

Kapatral, V., Campbell, J.W., Minnich, S.A., Thomson, N.R., Matsumura, P., and Pruss, B.M. (2004). Gene array analysis of *Yersinia enterocolitica* FlhD and FlhC: regulation of enzymes affecting synthesis and degradation of carbamoylphosphate. Microbiology *150*, 2289–2300.

Kapatral, V., Olson, J.W., Pepe, J.C., Miller, V.L., and Minnich, S.A. (1996). Temperature-dependent regulation of *Yersinia enterocolitica* Class III flagellar genes. Mol. Microbiol. *19*, 1061–1071.

Karlinsey, J.E., Lonner, J., Brown, K.L., and Hughes, K.T. (2000). Translation/secretion coupling by type III secretion systems. Cell *102*, 487–497.

Keseler, I.M., Mackie, A., Santos-Zavaleta, A., Billington, R., Bonavides-Martínez, C., Caspi, R., Fulcher, C., Gama-Castro, S., Kothari, A., Krummenacker, M., et al. (2017). The EcoCyc database: reflecting new knowledge about *Escherichia coli* K-12. Nucleic Acids Res. *45*, D543–D550.

Kitagawa, R., Takaya, A., and Yamamoto, T. (2011). Dual regulatory pathways of flagellar gene expression by ClpXP protease in enterohaemorrhagic *Escherichia coli*. Microbiology *157*, 3094–3103.

Kutsukake, K., Minamino, T., and Yokoseki, T. (1994). Isolation and characterization of FliK-independent flagellation mutants from *Salmonella typhimurium*. J. Bacteriol. *176*, 7625–7629.

Lam, O., Wheeler, J., and Tang, C.M. (2014). Thermal control of virulence factors in bacteria: a hot topic. Virulence *5*, 852–862.

Li, H., and Sourjik, V. (2011). Assembly and stability of flagellar motor in *Escherichia coli*. Mol. Microbiol. *80*, 886–899.

Lucchini, S., McDermott, P., Thompson, A., and Hinton, J.C. (2009). The H-NS-like protein StpA represses the RpoS (sigma 38) regulon during exponential growth of *Salmonella typhimurium*. Mol. Microbiol. *74*, 1169–1186.

Macnab, R.M. (2004). Type III flagellar protein export and flagellar assembly. Biochim. Biophys. Acta *1694*, 207–217.

Minnich, S.A., and Rohde, H.N. (2007). A rationale for repression and/or loss of motility by pathogenic Yersinia in the mammalian host. Adv. Exp. Med. Biol. *603*, 298–310.

Moliere, N., Hossmann, J., Schafer, H., and Turgay, K. (2016). Role of Hsp100/Clp protease complexes in controlling the regulation of motility in *Bacillus subtilis*. Front. Microbiol. *7*, 315.

Ni, B., Ghosh, B., Paldy, F.S., Colin, R., Heimerl, T., and Sourjik, V. (2017). Evolutionary remodeling of bacterial motility checkpoint control. Cell Rep. *18*, 866–877.

Nuss, A.M., Heroven, A.K., Waldmann, B., Reinkensmeier, J., Jarek, M., Beckstette, M., and Dersch, P. (2015). Transcriptomic profiling of *Yersinia pseudotuberculosis* reveals reprogramming of the Crp regulon by temperature and uncovers Crp as a master

regulator of small RNAs. PLoS Genet. *11*, e1005087.

Ottemann, K.M., and Miller, J.F. (1997). Roles for motility in bacterial-host interactions. Mol. Microbiol. *24*, 1109–1117.

Pesavento, C., Becker, G., Sommerfeldt, N., Possling, A., Tschowri, N., Mehlis, A., and Hengge, R. (2008). Inverse regulatory coordination of motility and curli-mediated adhesion in *Escherichia coli*. Gene Dev. *22*, 2434–2446.

Poblete-Castro, I., Escapa, I.F., Jager, C., Puchalka, J., Lam, C.M., Schomburg, D., Prieto, M.A., and Martins dos Santos, V.A. (2012). The metabolic response of P. putida KT2442 producing high levels of polyhydroxyalkanoate under single- and multiple-nutrient-limited growth: highlights from a multi-level omics approach. Microb. Cell Fact. *11*, 34.

Pruss, B.M. (2017). Involvement of two-component signaling on bacterial motility and biofilm development. J. Bacteriol. *199*, e00259–17.

Renault, T.T., Abraham, A.O., Bergmiller, T., Paradis, G., Rainville, S., Charpentier, E., Guet, C.C., Tu, Y., Namba, K., Keener, J.P., et al. (2017). Bacterial flagella grow through an injection-diffusion mechanism. Elife *6*, e23136.

Roncarati, D., and Scarlato, V. (2017). Regulation of heat-shock genes in bacteria: from signal sensing to gene expression output. FEMS Microbiol. Rev. *41*, 549–574.

Rosen, R., and Ron, E.Z. (2002). Proteome analysis in the study of the bacterial heat-shock response. Mass Spectrom. Rev. *21*, 244–265.

Schulmeister, S., Grosse, K., and Sourjik, V. (2011). Effects of receptor modification and temperature on dynamics of sensory complexes in *Escherichia coli* chemotaxis. BMC Microbiol. *11*, 222.

Shi, W., Li, C., Louise, C.J., and Adler, J. (1993). Mechanism of adverse conditions causing lack of flagella in *Escherichia coli*. J. Bacteriol. *175*, 2236–2240.

Siryaporn, A., Kim, M.K., Shen, Y., Stone, H.A., and Gitai, Z. (2015). Colonization, competition, and dispersal of pathogens in fluid flow networks. Curr. Biol. *25*, 1201–1207.

Soutourina, O.A., and Bertin, P.N. (2003). Regulation cascade of flagellar expression in Gram-negative bacteria. FEMS Microbiol. Rev. *27*, 505–523.

Wosten, M.M., van Dijk, L., Veenendaal, A.K., de Zoete, M.R., Bleumink-Pluijm, N.M., and van Putten, J.P. (2010). Temperature-dependent FlgM/FliA complex formation regulates *Campylobacter jejuni* flagella length. Mol. Microbiol. *75*, 1577–1591.

Supplemental Information

Inefficient Secretion of Anti-sigma

Factor FlgM Inhibits Bacterial

Motility at High Temperature

Iaroslav Rudenko, Bin Ni, Timo Glatter, and Victor Sourjik
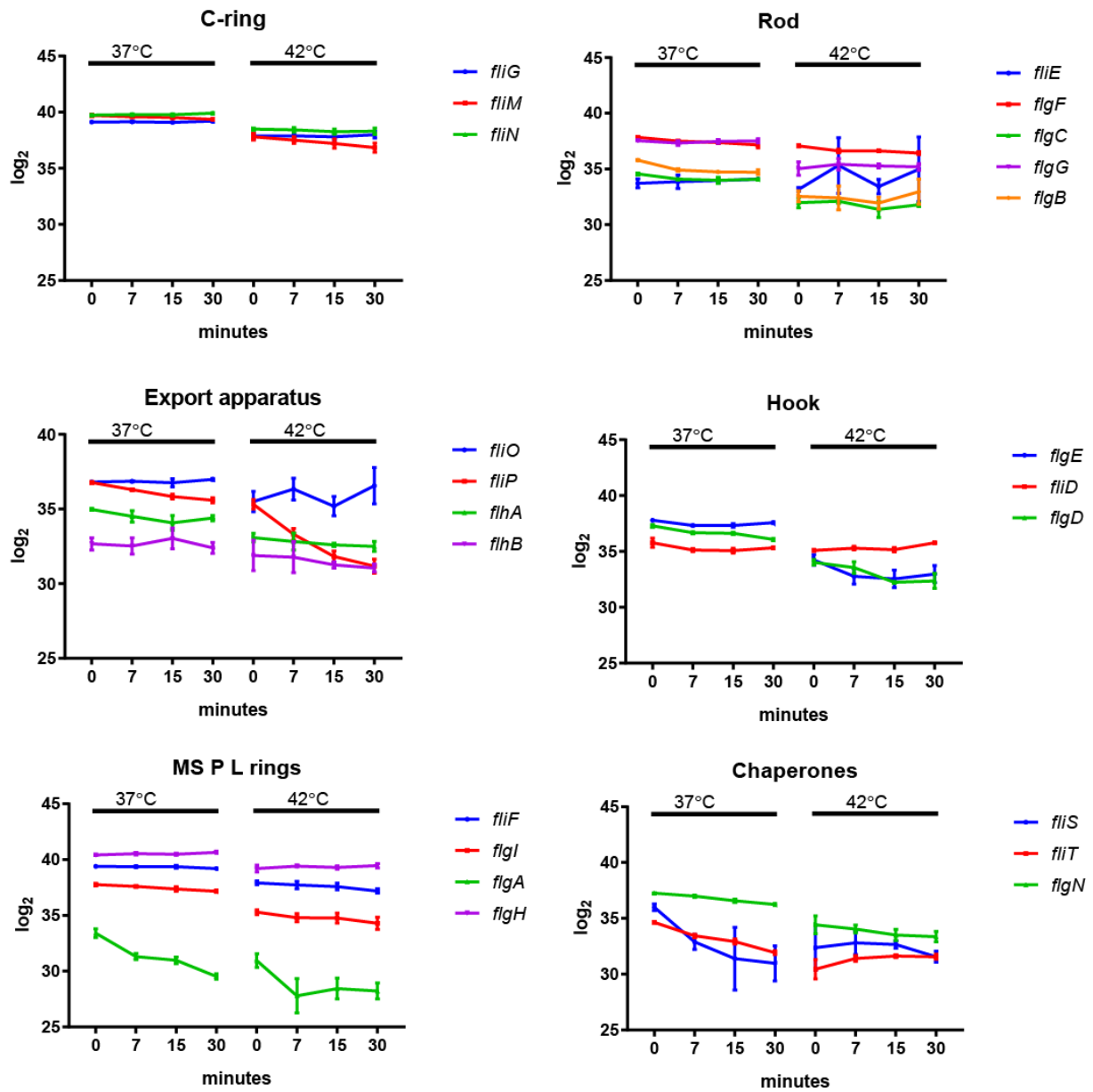
Figure S1. Effect of growth temperature on stability of flagellar components, Related to Figure 3.

Levels of indicated flagellar proteins were determined by mass spectrometry after translation was stopped by addition of 200 µg/ml chloramphenicol to cultures grown at 37°C (left) or at 42°C (right).
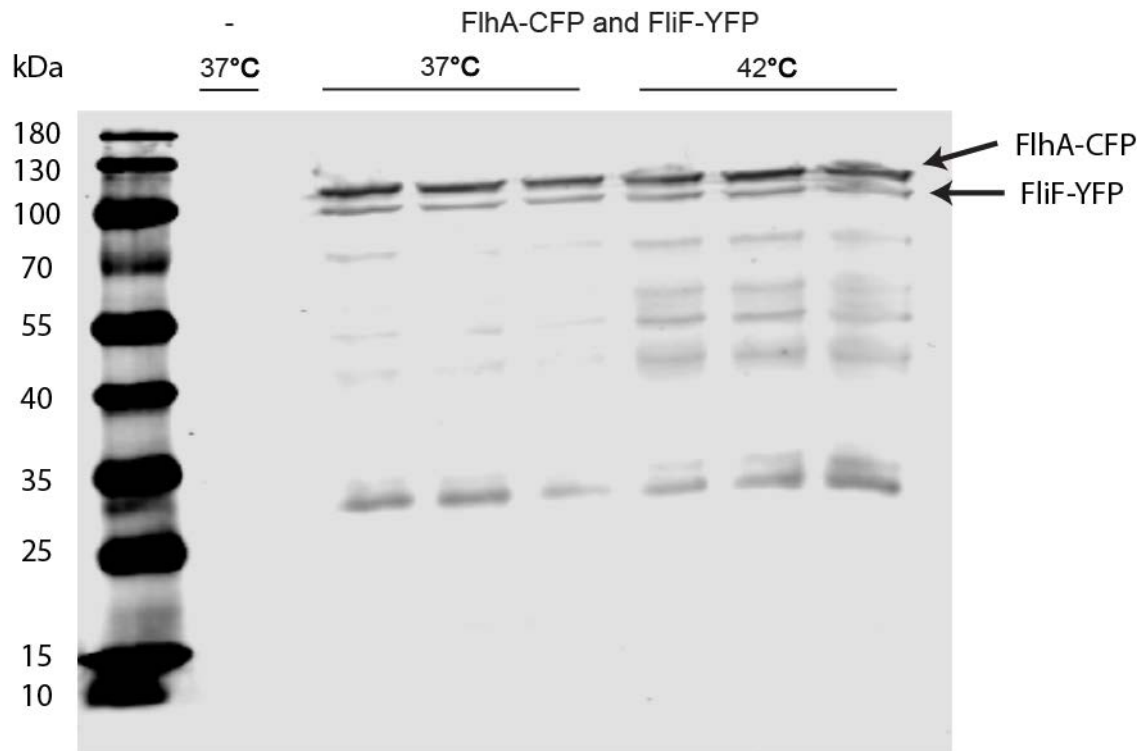
Figure S2. Immunoblot analysis of intracellular levels of FlhA-CFP and FliF-YFP at 37°C and 42°C, Related to Figure 4.

Cells expressing FliF-YFP from an IPTG-inducible plasmid and FlhA-CFP from an arabinose-inducible plasmid were grown in TB supplemented with 30 µM IPTG and 0.01% arabinose at either 37°C or 42°C. Immunoblot shows data from three independent experiments. Negative control (indicated by "-") shows cells without the plasmid. Tagged proteins were detected with Clontech Living Colors JL8 mouse anti-GFP antibody, diluted 1:10000).

Figure S3. Increased growth temperature affects localization of FliF and FlhA, Related to Figure 4.

Localization of FliF-YFP and FlhA-CFP in cells grown at 37°C (left) and 42°C (right), respectively. Enlarged images of the same experiment are shown in Figure 4A.
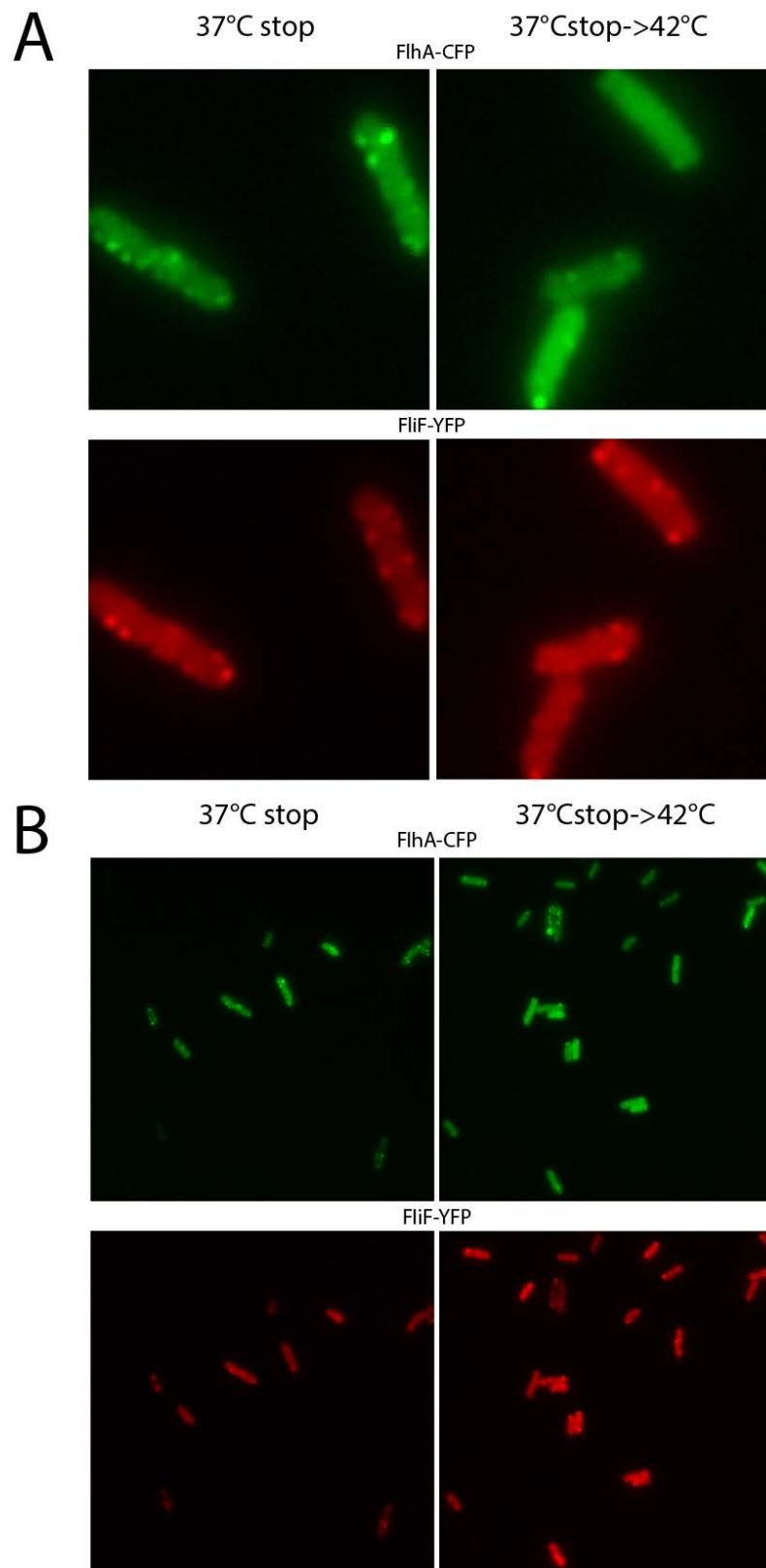
Figure S4. Effect of temperature on localization of FliF and FlhA in non-growing cells, Related to Figure 4.

(A) Localization of FliF-YFP and FlhA-CFP in cells grown at 37°C to OD_{600}=0.6 and subsequently incubated for 60 minutes with chloramphenicol (200 µg/ml final concentration) at 37°C (left) or at 42°C (right).

(B) Enlarged images of the same experiment.
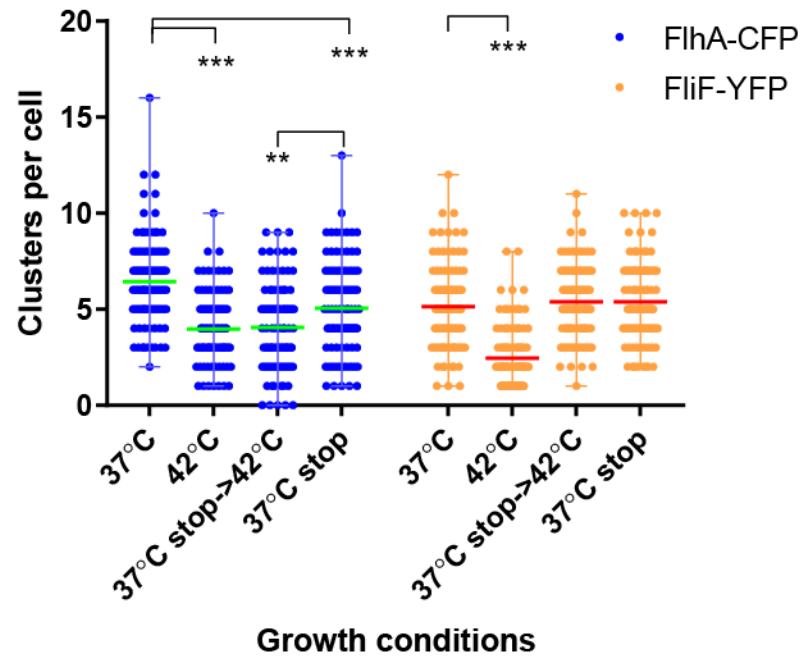
Figure S5. Effect of temperature on distribution of the FlhA and FliF clusters in growing and non-growing cells, Related to Figure 4.

Quantification of numbers of FlhA and FliF clusters per cell from experiments done as in Figures 4A, S3 and S4 (two independent experiments, blind count with overall 100 cells being quantified per each condition). Wide horizontal lines indicate the median. Asterisks indicate *P* value <0.0001 (***) and <0.004 (**).

SUPPLEMENTAL TABLES

Table S1. Transcriptome and proteome of *E. coli* at 37°C and 42°C (separate file), Related to Figure 1.

Table S2. Genes and proteins differentially regulated at 37°C and 42°C, Related to Figure 1.

List	Function	Genes
Downregulated at both levels	Motility	*aer cheA cheB cheR cheW cheY cheZ flgA flgB flgC flgD flgE flgG flgH flgI flgL flgN flhA flhE fliC fliF fliG fliH fliI fliL fliM fliN fliO fliP fliS fliT fliZ motA motB tap tar trg tsr ycgR yhjH*
	Possibly motility-related (FlhDC-controlled)	*yecR yjcZ ynjH modA modC*
	Arginine metabolsim	*astA astB astC astD astE*
		dmlA dppD dppF fecA gabT iraP lsrG ompF paaJ paaK patA puuA puuD ydcS yecC yhcN
Upregulated at both levels	Ribose metabolism	*rbsA rbsB rbsC rbsD rbsK*
		hchA lysA pfkB tdcB tdcG ygbM ykgE ykgF
Upregulated at mRNA level, downregulated at protein level		*fhuD fhuE gudD malK malP*
Downregulated at mRNA level, upregulated at protein level	Possibly motility-related (FlhDC-controlled)	*flxA*
Upregelated at protein level, unaffected at mRNA level		*araG ivy mscM stpA trpC yffR*
Downregulated at protein level, unaffected at mRNA level		*actP bcsG cyoB dctA dppA emtA fecE gabD gatY gcd gdhA glgP ilvN kgtP mhpR mtlR oppA oppC rhlE rpoS thrA ybdD ydcP ydiH yebV yjcH yjhU yjiY*
Upregulated at mRNA level, unaffected at protein level		*bioA borD carA carB evgA fhuA fhuC glcB livK lldD lldP lldR lrhA lysU mqo murQ nanC ompC psuG rcnB rstA sufA tdcE tonB treB treC yddB yibT*
Downregulated at mRNA level, unaffected at protein level		*artJ deaD flgF fliD fliY glcC katE lsrB lsrF osmC paaY prpD sdiA yqjI*

Table S3. mRNA levels of motility genes at different temperatures, Related to Figure 2.

Class 1

Name	27°C	32°C	37°C	42°C	37°/42° fold change
flhC	7.62732	8.24066	8.66601	8.55266	-1.081
flhD	7.84301	8.27317	8.72086	8.67868	-1.029

Class 2

Name	27°C	32°C	37°C	42°C	37°/42° fold change
flgA	7.63461	8.34928	9.17149	8.13027	-2.057*
flgB	9.54082	10.00423	10.90565	9.44529	-2.751*
flgC	10.14684	10.53449	11.44299	9.84394	-3.029*
flgD	10.35004	10.75795	11.53833	9.75153	-3.450*
flgE	10.68758	10.99807	11.79211	9.86462	-3.803*
flgF	10.3598	10.66854	11.46981	9.38931	-4.229*
flgG	10.18702	10.40821	11.17241	9.05731	-4.332*
flgH	9.12233	9.59102	10.43516	8.32885	-4.305*
flgI	8.56168	9.0471	9.92241	7.86455	-4.163*
flgJ	8.09503	8.77289	9.49319	7.47257	-4.057*
flgK	9.30507	9.70597	9.89308	7.30647	-6.006*
flgL	9.62154	9.84574	9.97963	7.36618	-6.119*
flhA	7.22139	7.98527	9.1346	7.3402	-3.468*
flhB	6.2417	7.28013	8.25015	6.89563	-2.557*
flhE	6.46765	7.24468	8.39182	6.62353	-3.406*
fliA	9.26029	9.9292	10.38504	8.94968	-2.704*
fliE	7.32818	8.12165	8.99634	7.38951	-3.045*
fliF	7.95739	9.00482	10.05396	8.52286	-2.890*
fliG	8.50554	9.40975	10.36234	8.47852	-3.690*
fliH	8.46907	9.44035	10.21594	8.39142	-3.541*
fliI	7.89988	8.70332	9.4911	7.62001	-3.658*
fliJ	7.49265	8.13873	8.94696	6.98907	-3.884*
fliK	7.66295	8.24861	8.93731	7.02272	-3.770*
fliL	8.6699	9.36462	10.33373	9.04849	-2.437*
fliM	8.58312	9.46241	10.33824	9.00056	-2.527*
fliN	8.70188	9.3638	10.2879	8.71568	-2.973*
fliO	8.20937	9.00751	9.93993	8.34937	-3.011*
fliP	7.20503	8.06545	9.13869	7.49554	-3.123*
fliQ	6.66176	7.55203	8.55515	6.92431	-3.096*
fliR	5.72879	6.75647	7.67678	6.2351	-2.716*
fliY	9.03639	9.39593	9.51851	8.12943	-2.619*

Class 2/3

Name	27°C	32°C	37°C	42°C	37°/42° fold change
flgM	9.55067	9.82614	10.00111	7.99745	-4.010*
flgN	9.21624	9.63381	9.72481	7.85936	-3.643*
fliD	8.71407	9.06827	9.32287	6.45432	-7.303*
fliS	8.33388	8.79075	9.12536	6.17149	-7.748*
fliT	8.25346	8.7871	9.112	6.2255	-7.394*
fliZ	8.27766	8.90633	9.3319	7.8229	-2.846*

Class 3

Name	27°C	32°C	37°C	42°C	37°/42° fold change
aer	8.33449	8.98442	9.08885	6.35121	-6.669*
cheA	8.84882	9.19104	9.21703	5.6256	-12.053*
cheB	8.63645	8.76079	8.79877	5.03994	-13.536*
cheR	8.90071	9.15621	9.08442	5.2716	-14.053*
cheW	9.68908	9.67268	9.6708	6.10183	-11.867*
cheY	9.71573	9.76214	9.68469	6.10027	-11.995*
cheZ	9.49284	9.54679	9.43997	6.0658	-10.368*
fliC	13.32401	13.39511	13.43641	9.35687	-16.906*
motA	9.42471	9.89851	9.79141	6.14345	-12.535*
motB	9.0041	9.4676	9.37511	5.7102	-12.683*
tap	9.75504	9.95188	9.76743	5.82412	-15.383*
tar	9.76561	9.83737	9.49874	5.6882	-14.030*
trg	8.64674	8.87764	8.61635	6.88406	-3.322*
tsr	9.15564	9.37628	9.46328	5.90916	-11.746*

* Statistical significance was determined using the Holm-Sidak method, with alpha = 0.05.
Each row was analyzed individually, without assuming a consistent SD

Table S4. Levels of motility proteins at 37°C and 42°C, Related to Figure 2.

Class 1

Name	37°C	SD	42°C	SD	37°/42° fold change
FlhD	36.72835	±0.19908	35.66503	±0.06892	-2.12664*

Class 2

Name	37°C	SD	42°C	SD	37°/42° fold change
FlgA	33.4075	±0.390231	30.95003	±0.600723	-4.91495*
FlgB	35.79425	±0.039137	32.54871	±0.489929	-6.49109*
FlgC	34.55491	±0.08604	31.96828	±0.453468	-5.17326*
FlgD	37.28481	±0.108998	34.02745	±0.250561	-6.51472*
FlgE	37.79039	±0.069392	34.24257	±0.489394	-7.09564*
FlgF	37.84097	±0.028202	37.06837	±0.085682	-1.54519*
FlgG	37.5389	±0.018912	35.03044	±0.604059	-5.01693*
FlgH	40.40107	±0.044832	39.19831	±0.311604	-2.40553*
FlgI	37.39599	±0.062455	34.40637	±0.462024	-5.97923*
FlgK	36.4461	±0.186896	38.23727	±1.767413	3.582337
FlgL	36.03459	±0.153546	30.8596	±1.366443	-10.35*
FlhA	34.97187	±0.058257	33.08012	±0.289376	-3.7835*
FlhB	32.66515	±0.408911	31.88666	±1.014674	-1.55698
FlhE	35.93712	±0.043759	33.74956	±0.629235	-4.37511*
FliA	39.06175	±0.06072	38.90281	±0.132525	-0.31788
FliE	33.71065	±0.390173	33.16623	±0.16755	-1.08885
FliF	39.39853	±0.112636	37.91434	±0.180071	-2.96838*
FliG	39.11958	±0.057142	37.87611	±0.239132	-2.48695*
FliH	36.24588	±0.058917	32.23889	±0.475998	-8.01399*
FliI	37.7511	±0.089762	35.2885	±0.220097	-4.92521*
FliJ	33.29623	±0.254312	33.19172	±0.39015	-0.20903
FliL	39.78004	±0.043225	38.76131	±0.200102	-2.03747*
FliM	39.70889	±0.082973	37.8165	±0.28949	-3.78478*
FliN	39.74184	±0.031097	38.4961	±0.097766	-2.49148*
FliO	36.81225	±0.076642	35.49867	±0.674122	-2.62717
FliP	36.77156	±0.056653	35.32002	±0.310748	-2.90306*

Class 2/3

Name	37°C	SD	42°C	SD	37°/42° fold change
FliD	35.78211	±0.40398	35.09554	±0.03006	-1.37314
FliS	35.98874	±0.29766	32.38306	±2.02655	-7.21137
FliT	34.64975	±0.08518	30.43966	±0.86336	-8.42019*
FliZ	37.92451	±0.20691	36.16139	±0.14262	-3.52623*
FlgM	39.33072	±0.05324	39.38310	±0.11972	0.10476
FlgN	37.25142	±0.03550	34.42592	±0.80228	-5.65101*

* Statistical significance was determined using the Holm-Sidak method, with alpha = 0.05.
Each row was analyzed individually, without assuming a consistent SD

TRANSPARENT METHODS

Bacterial strains, media and growth conditions

Experiments were performed in *E. coli* strain MG1655. *ΔflgM* knockout strain was made by P1 transduction using strains from the Keio collection (Baba et al., 2006) as donors. FLP recombinase expressed from the plasmid pCP20 (Cherepanov and Wackernagel, 1995) was used to excise the kanamycin cassette. For experiments with planktonic cultures, overnight cultures were inoculated from glycerol stock and grown at 37°C on a rotary wheel in 5 ml TB (1% tryptone and 0.5% NaCl) supplemented with appropriate antibiotics. Overnight cultures were diluted 1:100 in 25 ml fresh TB supplemented with appropriate antibiotics and Isopropyl β-D-1-thiogalactopyranoside (IPTG) for induction, when necessary. Unless stated otherwise, cells were grown at either 37°C or 42°C and 250 rpm (orbital shaker) until they reached optical density at 600 nM (OD_{600})=0.6 (Ultrascpec 10, Amersham Biosciences) and used for further experiments.

Total RNA isolation and analysis of gene expression

Cells were grown in 25 ml TB until OD_{600}=0.6, harvested by centrifugation and proceeded according to the manufacturer's instructions for GeneMATRIX Universal RNA Purification Kit (including on-column DNAse digestion). Quality of the isolated RNA was examined by agarose gel electrophoresis and samples were sent to the Max Planck-Genome-centre (Cologne). Obtained FASTA files were mapped to the genome of *E. coli* MG1655 (excluding rRNA and tRNAs) using DNAStar ArrayStar (Madison, Wisconsin USA). The analysis of the transcriptomic data was performed using DNAStar ArrayStar. All datasets were capped to the auto-calculated minimum value and normalized by assigning Reads per Kilobase of template per Million mapped reads (RPKM). Replicates of the experiments were averaged to mean values. If not indicated otherwise, genes were considered as differentially regulated if they exhibited more than 2-fold change and over 90% confidence (Student's t-test, Benjamini and Hochberg). Initial clustering of the genes based on their expression profiles was performed using built-in *k*-means clustering algorithm (default parameters), Standard Pearson distance metric. Gene Ontology annotation was downloaded from PortEco (Hu et al., 2014). Expression profiles of genes and proteins were visualized in Microsoft Excel and GraphPad Prism (GraphPad Software, San Diego, California, USA).

Total proteomic analysis using data independent acquisition-mass spectrometry (DIA-MS)

Cells were grown at indicated temperature in TB until OD_{600}=0.6 at 250 rpm, harvested by centrifugation and processed as described (Yuan et al., 2017). For the translation stop experiments, chloramphenicol was added to the culture at OD_{600}=O.6 to the final concentration of 200 mg/ml, samples were taken at time points 0, 7, 15 and 30 minutes and proceeded as described above. Pellets containing lyophilized peptides were analyzed by mass spectrometry by the Proteomic Core facility of the MPI for Terrestrial Microbiology.

E. coli cell pellets were treated according to the method described in (Yuan et al., 2017) with some modifications. Cell pellets were resuspended in lysis buffer containing 0.5% sodium lauroyl sarcosinate (SLS) in 100 mM ammonium bicarbonate. Cells were lysed by incubation at 95°C for

15min and sonication (Vial Tweeter, Hielscher). Cell lysates were then reduced by adding 5 mM Tris(2-caboxyethyl)phosphine and incubation at 95°C for 15 minutes, followed by alkylation (10mM iodoacetamide, 30min at 25°C). Lysates were cleared by centrifugation and the total protein was estimated for each sample with Pierce™ BCA Protein Assay Kit (ThermoFisher Scientific). 50 µg total protein was then digested with 1 µg trypsin (Promega) overnight at 30°. Next, SLS was precipitated with 1.5% trifluoroacetic acid (TFA) and peptides were purified using C18 microspin columns according to the manufacturer's instruction (Harvard Apparatus). In order to generate an in-depth project specific *E.coli* spectral library for subsequent DIA analysis, a peptide pool was generated to prepare an *E. coli* spectral library. For this one aliquot of each sample condition was mixed and separated on a microspin column using high pH into 6 fractions (strategy adopted from (Yang et al., 2012) Peptides were dried, reconstituted in 0.1% TFA and mixed with iRT retention time calibration peptides (Biognosys).

Peptide mixtures were then analyzed using liquid chromatography-mass spectrometry carried out on a Q-Exactive Plus instrument connected to an Ultimate 3000 RSLC nano with a Prowflow upgrade and a nanospray flex ion source (all Thermo Scientific). Peptide separation was performed on a reverse phase HPLC column (75 µm x 42 cm) packed in-house with C18 resin (2.4 µm, Dr. Maisch). The following separating gradient was used: 95% solvent A (0.15% formic acid) and 5% solvent B (99.85% acetonitrile, 0.15% formic acid) to 20% solvent B over 60 minutes and to 35% B for additional 30 minutes at a flow rate of 300 nl/min. DIA-MS acquisition method was adapted from (Bruderer et al., 2015). In short, one full MS scan was performed using the a scan range of 375-1500 m/z, automatic gain control (AGC) was set to $3x10^6$ and the ion accumulation time 120ms with a resolution of 70.000 K width at half maximum (at m/z 200). For each MS1 scan, 19 DIA windows with window sizes according to (Bruderer et al., 2015) were acquired. DIA acquisition parameters were set to 35.000 K resolution, ACG target settings $3x10^6$, 120ms ion accumulation time. Fragmentation was initiated with stepped collision energy of 22.5, 25, 27.5.

For spectral library generation data dependent acquisition mass spectrometry (DDA-MS) was performed on the individual peptide fractions. DDA scans were obtained by one high resolution MS scan at a resolution of 70,000 full width at half maximum (at *m/z* 200) followed by MS/MS scans of the 10 most intense ions. To increase the efficiency of MS/MS attempts, the charged state screening modus was enabled to exclude unassigned and singly charged ions. The dynamic exclusion duration was set to 30 seconds. The ion accumulation time was set to 50 ms for MS and 50 ms at 17,500 resolution for MS/MS. The automatic gain control was set to $3x10^6$ for MS survey scans and $1x10^5$ for MS/MS scans.

MS/MS searches of DDA raw data were performed using MASCOT (Version 2.5, Matrix Science) submitted from the Proteome Discoverer (v.1.4, Thermo Scientific) software environment. Modifications were set as follows: carbamidomethylation of cysteines as fixed, oxidation of methionines and deamidation of glutamines and asparagines as variable. Spectral libraries were then generated within Spectronaut (v.11, Biognosys) with standard settings.

All DIA data were analyzed using Spectronaut (v.11, Biognosys) in default settings. DIA data was exported from Spectronaut and then used for further data extraction.

Experiments were performed in triplicates; data significance was calculated using multiple *t*-test comparison built-in the GraphPad Prism v7.03 (one unpaired *t*-test per row, each row analyzed individually. For the data shown in Figure 1 and Table S2, consistent standard deviation was not assumed, desired false discovery rate (FDR) was set to 10% (Benjamini and Hochberg). Proteins were considered as differentially regulated if they exhibited more than 2-fold change. Mapping of transcriptomic and proteomic data was performed using Cytoscape v 3.2.1 (Shannon et al., 2003). The rate of protein degradation was compared using a linear fit, calculated in the GraphPad Prism v7.03. Each replicate was considered as an individual point, slopes were considered different when 95% confidence intervals (CI) did not overlap.

Secretion assay

For the secretion assay, *E. coli* MG1655 strains, containing FlgM-HA or FliC-HA on IPTG-inducible plasmid (Ni et al., 2017) were inoculated in 25 ml TB, supplemented with 100µM IPTG and were grown at 37°C or 42°C as described above. To measure intracellular protein level, 1 ml of cell culture was centrifuged at maximum speed (table top centrifuge) To measure the concentration of the secreted protein in the cultural liquid, 20 ml of culture (OD_{600}=0.6) were supplemented with 5 ml TCA and centrifuged 30 minutes at 4°C. Pellets were washed with 5 ml of 100% acetone (vortexed, centrifuged 10 minutes at 4°C). Pellets were dried under the hood to remove the residual acetone; proteins were dissolved in SDS sample buffer, loaded on the SDS gel and transferred on the nitrocellulose membrane using standard Western Blot protocol. Detection was performed with mouse α-HA antibodies (dilution 1:10 000, Sigma-Aldrich) and IRD-labelled goat α-mouse antibodies (dilution 1:5 000, IRDye 700 DX). Light signals were detected using LiCor ODYSSEY CLx and analyzed using Image Studio v 5.2.

Analysis of promotor activity

Flow cytometry was used to monitor activity of promoters for *flhD* (class I), *fliE* (class II) and *fliC* (class III) using GFP-reporters (Zaslaver et al., 2006). Cells were grown as described above. Fluorescence-activated cell analysis (20 µl of culture were inoculated in 2 ml of Tethering buffer, 10,000 cells per sample acquired) was carried out on a BD LSR Fortessa SORP flow-cytometer (BD Biosciences). GFP was excited using a 488-nm laser (blue) at 100 mW for excitation and a 510/20 bandpass filter. The acquired data was analyzed using BD FACS Diva software (BD Biosciences). For all reporters, at least three independent biological replicates were used for quantification.

Fluorescence microscopy

Microscopy measurements were performed as described previously (Li and Sourjik, 2011). Cells were grown as above at either 37°C or 42°C in TB containing 0.01% arabinose and 30 µM IPTG to respectively induce expression of FlhA-CFP and FliF-YFP. Where indicated, chloramphenicol has been added at final concentration of 200 µg/ml to inhibit protein synthesis. Stability of full-length protein fusions was confirmed using Western Blot with Clontech Living Colors JL8 mouse anti-GFP antibody and IRD-labelled goat α-mouse antibodies. For microscopy, 3 µl of cell culture was pipetted onto a thin pad of 1% agarose. Fluorescence images were acquired on a Zeiss AxioImager

microscope equipped with an ORCA AG CCD camera (Hamamatsu), a 100x oil objective (NA 1.45), and HE YFP (excitation bandpass 500/25, emission 535/30) and HE CFP (excitation 436/25, emission 480/40) filter sets. Each imaging experiment was performed in duplicate on independent cultures. All images were acquired under identical conditions. Images were subsequently analyzed using ImageJ software. Clusters were counted manually (blind count) using in total 10 independent images for each condition obtained during two independent experiments. 10 cells per image were used for cluster count. Both FlhA-CFP and FliF-YFP clusters were counted in same cells (100 individual cells from 10 different images in total per condition). Significance was calculated using unpaired non-parametric t-test (Mann-Whitney) with exact two-tailed P value. *** indicate P value <0.0001, ** indicate P value <0.005.

Swimming velocity measurement

Cell cultures were grown in TB at 37 or 42°C with shaking (150 rpm) as indicated. When OD_{600} reached 0.5-0.6, cell cultures were mixed with two volume of tethering buffer. Swimming velocity was measured by tracking cells in a poly-dimethylsiloxane (PDMS) microchamber using phase-contrast microscopy (Nikon TI Eclipse, 10x objective with NA = 0.3, CMOS camera EoSens 4CXP). All data were analyzed with ImageJ (https://imagej.nih.gov/ij/) by using custom-written plugins. For swimming velocity analysis during temperature transition, cell cultures were grown as above, and when OD_{600} reached 0.6 the temperature for growth was changed from 42 to 37°C.

Flagellar length and number quantification

Bacteria were grown in TB at 37 or 42°C with shaking (150 rpm). When cell density (OD_{600}) reached 0.6, 5 µL cell suspensions were applied onto hydrophilized carbon-coated copper grids (400 mesh). After a short wash step with PBS and water, bacterial cells were stained with 2% uranyl acetate. All samples were analyzed with a JEOL JEM-2100 transmission electron microscope by using an acceleration voltage of 120 kV. For image acquisition, F214 FastScan CCD camera (TVIPS; Gauting) was used. Flagellar number and length were analyzed with ImageJ.

DATA AND SOFTWARE AVAILIABILITY

RNA-seq data have been deposited in the ArrayExpress database at EMBL-EBI (www.ebi.ac.uk/arrayexpress) under accession number E-MTAB-7733. The mass spectrometry proteomics data have been deposited to the ProteomeXchange Consortium via the PRIDE partner repository (https://www.ebi.ac.uk/pride/archive/) with the dataset identifier PXD012611 and 10.6019/PXD012611.

SUPPLEMENTAL REFERENCES

Baba, T., Ara, T., Hasegawa, M., Takai, Y., Okumura, Y., Baba, M., Datsenko, K.A., Tomita, M., Wanner, B.L., and Mori, H. (2006). Construction of Escherichia coli K-12 in-frame, single-gene knockout mutants: the Keio collection. Mol syst biol *2*, 2006.0008.

Bruderer, R., Bernhardt, O.M., Gandhi, T., Miladinovic, S.M., Cheng, L.Y., Messner, S., Ehrenberger, T., Zanotelli, V., Butscheid, Y., Escher, C.*, et al.* (2015). Extending the limits of quantitative proteome profiling with data-independent acquisition and application to acetaminophen-treated three-dimensional liver microtissues. Mol cell proteomics : MCP *14*, 1400-1410.

Cherepanov, P.P., and Wackernagel, W. (1995). Gene disruption in Escherichia coli: TcR and KmR cassettes with the option of Flp-catalyzed excision of the antibiotic-resistance determinant. Gene *158*, 9-14.

Hu, J.C., Sherlock, G., Siegele, D.A., Aleksander, S.A., Ball, C.A., Demeter, J., Gouni, S., Holland, T.A., Karp, P.D., Lewis, J.E.*, et al.* (2014). PortEco: a resource for exploring bacterial biology through high-throughput data and analysis tools. Nucleic Acids Res *42*, D677-684.

Li, H., and Sourjik, V. (2011). Assembly and stability of flagellar motor in Escherichia coli. Mol microbiol *80*, 886-899.

Ni, B., Ghosh, B., Paldy, F.S., Colin, R., Heimerl, T., and Sourjik, V. (2017). Evolutionary Remodeling of Bacterial Motility Checkpoint Control. Cell rep *18*, 866-877.

Shannon, P., Markiel, A., Ozier, O., Baliga, N.S., Wang, J.T., Ramage, D., Amin, N., Schwikowski, B., and Ideker, T. (2003). Cytoscape: a software environment for integrated models of biomolecular interaction networks. Genome res *13*, 2498-2504.

Yang, F., Shen, Y., Camp, D.G., 2nd, and Smith, R.D. (2012). High-pH reversed-phase chromatography with fraction concatenation for 2D proteomic analysis. Expert rev proteomic *9*, 129-134.

Yuan, J., Jin, F., Glatter, T., and Sourjik, V. (2017). Osmosensing by the bacterial PhoQ/PhoP two-component system. P Natl Acad Sci USA *114*, E10792-e10798.

Zaslaver, A., Bren, A., Ronen, M., Itzkovitz, S., Kikoin, I., Shavit, S., Liebermeister, W., Surette, M.G., and Alon, U. (2006). A comprehensive library of fluorescent transcriptional reporters for Escherichia coli. Nat methods *3*, 623-628.